

On the Effect of Electron-Phonon Interaction Parameters on the Performance of Carbon Nanotube Based Transistors

M. Pourfath and H. Kosina

Institute for Microelectronics, TU Wien, Gußhausstraße 27–29/E360, A-1040 Wien, Austria

email: pourfath@iue.tuwien.ac.at

Exceptional electronic and mechanical properties together with nanoscale diameter make carbon nanotubes (CNTs) promising candidates for nanoscale transistors. Semiconducting CNTs can be used as a channel for field-effect transistors (FETs), and metallic CNTs can serve as interconnect wires. In short devices carrier transport through the device is nearly ballistic [1].

The non-equilibrium Green's function (NEGF) method has been successfully utilized to investigate the characteristics of nanoscale Silicon transistors [2], carbon nanotube (CNT) based transistors [3, 4], and molecular devices [5]. In this work we employ the NEGF formalism to study in detail quantum transport in CNT based transistors.

Non-equilibrium statistical ensemble averages of the single particle correlation operator can be calculated using the NEGF formalism. Four types of Green's functions are defined: $G^{R,A}$ deal with the dynamics of carriers and $G^{<,>}$ with the statistics of carriers. For a steady state problem the Green's functions can be written as [6]:

$$G_{\mathbf{r},\mathbf{r}'}^{R,A}(E) = [EI - H_{\mathbf{r},\mathbf{r}'}(E) - \Sigma_{\mathbf{r},\mathbf{r}'}^{R,A}(E)]^{-1} \quad (1) \quad G_{\mathbf{r},\mathbf{r}'}^{<,>}(E) = G_{\mathbf{r},\mathbf{r}'}^R(E)\Sigma_{\mathbf{r},\mathbf{r}'}^{<,>}(E)G_{\mathbf{r},\mathbf{r}'}^A(E) \quad (2)$$

In (1) an effective mass Hamiltonian is assumed. A recursive Green's function method is used for solving (1) and (2), see [2]. We consider the self-energies due to contacts and electron-phonon interaction, $\Sigma = \Sigma_s + \Sigma_d + \Sigma_{e-ph}$. The self-energy due to the coupling of the device to the source and drain contacts is only non-zero at the boundaries. The self-energy due to electron-phonon interaction consists of the contributions of elastic and inelastic scattering mechanisms, $\Sigma_{e-ph} = \Sigma_{el} + \Sigma_{inel}$. Assuming local scattering ($\Sigma_{\mathbf{r},\mathbf{r}'} = 0$ for $\mathbf{r} \neq \mathbf{r}'$) the self-energies due to electron-phonon interaction are given by:

$$\Sigma_{inel,(\mathbf{r},\mathbf{r})}^{<}(E) = \sum_{\nu} D_{inel}^{\nu} [(n_B(\hbar\omega_{\nu}) + 1)G_{\mathbf{r},\mathbf{r}}^{<}(E + \hbar\omega_{\nu}) + n_B(\hbar\omega_{\nu})G_{\mathbf{r},\mathbf{r}}^{<}(E - \hbar\omega_{\nu})] \quad (3) \quad \Sigma_{el,(\mathbf{r},\mathbf{r})}^{<,>}(E) = D_{el}G_{\mathbf{r},\mathbf{r}}^{<,>}(E) \quad (4)$$

$$\Sigma_{inel,(\mathbf{r},\mathbf{r})}^{>}(E) = \sum_{\nu} D_{inel}^{\nu} [(n_B(\hbar\omega_{\nu}) + 1)G_{\mathbf{r},\mathbf{r}}^{>}(E - \hbar\omega_{\nu}) + n_B(\hbar\omega_{\nu})G_{\mathbf{r},\mathbf{r}}^{>}(E + \hbar\omega_{\nu})] \quad (5) \quad \Im m[\Sigma^R] = \frac{[\Sigma^{>} - \Sigma^{<}]}{2i} \quad (6)$$

where ν is the phonon mode and the phonon occupation number is given by the Bose-Einstein distribution function $n_B(\hbar\omega_{\nu}) = 1/(\exp(\hbar\omega_{\nu}/k_B T) - 1)$. The electron-phonon coupling coefficients ($D_{el,inel}$) depend on the chirality and the diameter of the CNT [7]. The imaginary part of the self-energy broadens the density of states and is given by (6). The carrier concentration and the current density at some point \mathbf{r} of the device can be calculated as (7) and (8).

$$n_{\mathbf{r}} = -4i \int G_{\mathbf{r},\mathbf{r}}^{<}(E) \frac{dE}{2\pi} \quad (7) \quad j_{\mathbf{r}} = \frac{4q}{\hbar} \int \text{Tr}[\Sigma_{\mathbf{r},\mathbf{r}}^{<}G_{\mathbf{r},\mathbf{r}}^{>}(E) - \Sigma_{\mathbf{r},\mathbf{r}}^{>}G_{\mathbf{r},\mathbf{r}}^{<}(E)] \frac{dE}{2\pi} \quad (8)$$

The effects of the electron-phonon coupling strength and the phonon energy on the static response of CNTFETs are investigated. All simulations were performed for the structure shown in Fig. 1. To compare the effect of different scattering mechanisms, we define the ballisticity as the ratio of the current in the presence of electron-phonon interaction to the current in the ballistic case (I_{Sc}/I_{Bl}). With increasing $D_{el,inel}$ the imaginary part of the self-energy increases, which adds dissipation to the Hamiltonian, and as a result the total current decreases. Fig. 2 shows the ballisticity versus $D_{el,inel}$. Elastic scattering conserves the energy of carriers as in the ballistic case, but the current decreases due to elastic back-scattering of carriers. With inelastic scattering the energy of carriers is not conserved. Carriers which acquire enough kinetic energy can emit phonons and scatter into lower energy states. Fig. 2 shows that the variation of ballisticity versus D_{inel} strongly depends on the phonon energy. For a better comparison Fig. 3 shows the ballisticity versus phonon energy. With the increase of phonon energy the ballisticity increases, since scattered carriers lose more kinetic energy and the probability for back-scattering decreases [8]. As the phonon energy increases the occupation number decreases exponentially. Therefore, the self-energy decreases and the current is weakly affected even for strong electron-phonon coupling. Fig. 2 and Fig. 3 show the results for a device with a length of 50 nm. As the length of the CNT increases the ballisticity of the devices decreases. Fig. 4 shows the ballisticity versus the device length. As one expects, the ballisticity is inversely proportional to the device length.

In general electron-phonon interaction parameters depends on the diameter and the chirality of the CNT. The calculation of these parameters is presented in [7]. In CNTs the band gap is inversely proportional to the diameter. A rough estimate is $E_g = 0.8 \text{ eV}/d_{CNT} \text{ nm}$. CNTs with a diameter $d_{CNT} > 2 \text{ nm}$ have a band gap $E_g < 0.4 \text{ eV}$, which render them unsuitable as channel for FETs. However, the fabrication of devices with a diameter $d_{CNT} < 1 \text{ nm}$ is very difficult. As a result, we limit our study to zigzag CNTs with diameters in the range $d_{CNT} = 1 - 2 \text{ nm}$.

In CNTs elastic scattering is caused by acoustic phonons and inelastic scattering occurs due to zone boundary (ZB), optical (OP), and radial breathing (RBM) phonon modes. Considering the class of CNTs we discussed above, the energies of these phonon modes are $\hbar\omega_{ZB} \approx 160$ and 180 meV , $\hbar\omega_{OP} \approx 200 \text{ meV}$, and $\hbar\omega_{RBM} \approx 30 \text{ meV}$ respectively [9]. The corresponding coupling coefficients are $D_{inel}^{ZB,OP} < 50 \times 10^{-3} \text{ eV}^2$ and $D_{inel}^{RBM} < 10^{-3} \text{ eV}^2$ [7, 9]. As we discussed, for short devices (less

than some hundred nano-meter) high energy phonons, such as OP and ZB phonon modes, degrade the performance only weakly, whereas the RBM phonon mode can have a detrimental effect. However, due to weak electron-phonon coupling the RBM mode has a negligible effect at room temperature. The electron-phonon coupling is also weak for acoustic phonon (AP) modes ($D_{el}^{AP} < 10^{-3} \text{ eV}^2$), which implies weak elastic backscattering of carriers. Therefore, short CNTFETs can operate close to the ballistic limit. Fig. 5 shows excellent agreement between simulation results and experimental data [1]. The result for the bias point $V_G = 1.3 \text{ V}$ is compared with the ballistic limit, which confirms the validity of nearly ballistic transport in short CNTFETs.

Based on the NEGF formalism we investigated the effect of electron-phonon interaction on the performance of CNTFETs. For elastic scattering the electron-phonon coupling strength plays an important role. For inelastic scattering not only the coupling strength, but also the phonon energy is an important factor. In CNTs relevant for FETs, either the electron-phonon coupling is weak or the phonon energies are high. Therefore, the performance of short devices is only weakly affected.

References

- [1] A. Javey *et al.*, Nano Lett. **4**, 1319 (2004).
- [2] A. Svizhenko *et al.*, J.Appl.Phys. **91**, 2343 (2002).
- [3] J. Guo, J.Appl.Phys. **98**, 063519 (2005).
- [4] A. Svizhenko *et al.*, Phys.Rev.B **72**, 085430 (2005).
- [5] W. Tian *et al.*, J.Chem.Phys **109**, 2874 (1998).
- [6] S. Datta, Superlattices & Microstructures **28**, 253 (2000).
- [7] G. Mahan, Phys.Rev.B **68**, 125409 (2003).
- [8] J. Guo *et al.*, Appl.Phys.Lett. **86**, 193103 (2005).
- [9] S. Koswatta *et al.*, cond-mat/0511723 (2005).

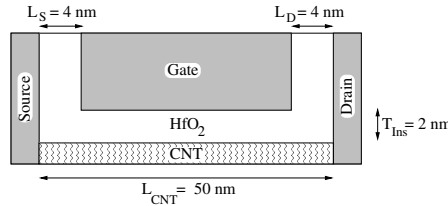


Figure 1: Sketch of the device. $T_{Ins} = 2 \text{ nm}$, $L_{CNT} = 50 \text{ nm}$ and $\epsilon_r = 15$.

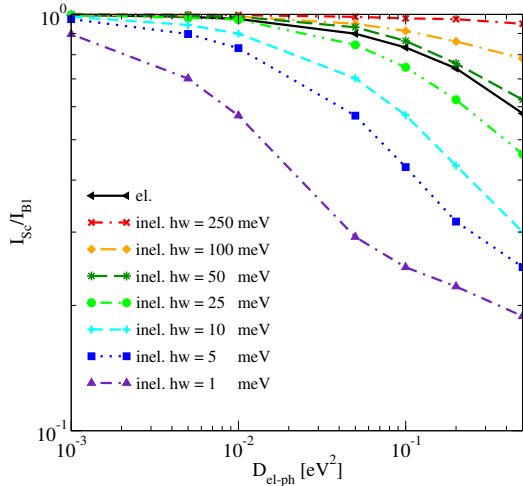


Figure 2: Ballistic current ratio I_{sc}/I_{BI} versus the strength of electron-phonon coupling ($D_{el,inel}$) for elastic and inelastic scattering.

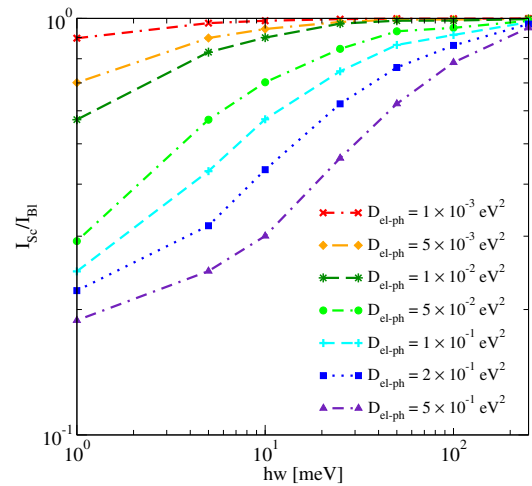


Figure 3: Ballistic current ratio I_{sc}/I_{BI} versus phonon energy ($\hbar\omega_\nu$) for inelastic scattering.

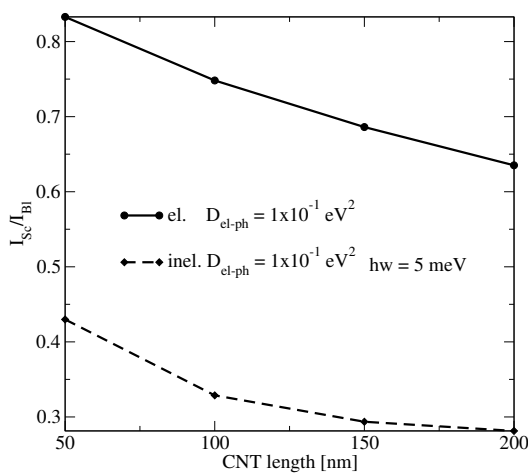


Figure 4: Ballistic current ratio I_{sc}/I_{BI} versus CNT length.

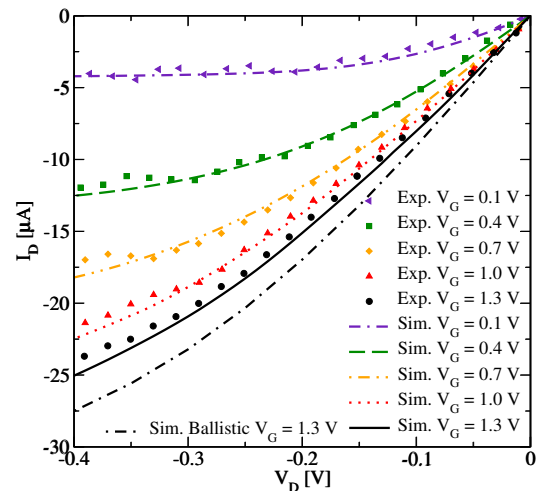


Figure 5: Comparison of the simulation results and experimental data for the output characteristics. The results for the bias point $V_G = 1.3 \text{ V}$ are compared with the ballistic limit.